

## Accepted Manuscript

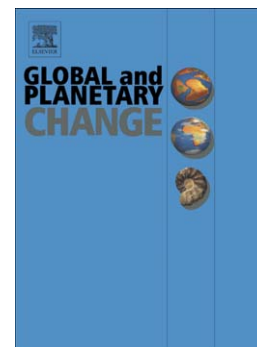
Glacioeustatic control on the origin and cessation of the Messinian salinity crisis

José N. Pérez-Asensio, Julio Aguirre, Gonzalo Jiménez-Moreno, Gerhard Schmiedl, Jorge Civis

PII: S0921-8181(13)00179-3  
DOI: doi: [10.1016/j.gloplacha.2013.08.008](https://doi.org/10.1016/j.gloplacha.2013.08.008)  
Reference: GLOBAL 2016

To appear in: *Global and Planetary Change*

Received date: 17 June 2013  
Revised date: 9 August 2013  
Accepted date: 12 August 2013



Please cite this article as: Pérez-Asensio, José N., Aguirre, Julio, Jiménez-Moreno, Gonzalo, Schmiedl, Gerhard, Civis, Jorge, Glacioeustatic control on the origin and cessation of the Messinian salinity crisis, *Global and Planetary Change* (2013), doi: [10.1016/j.gloplacha.2013.08.008](https://doi.org/10.1016/j.gloplacha.2013.08.008)

This is a PDF file of an unedited manuscript that has been accepted for publication. As a service to our customers we are providing this early version of the manuscript. The manuscript will undergo copyediting, typesetting, and review of the resulting proof before it is published in its final form. Please note that during the production process errors may be discovered which could affect the content, and all legal disclaimers that apply to the journal pertain.

**Glacioeustatic control on the origin and cessation of the Messinian salinity crisis**

José N. Pérez-Asensio<sup>a,\*</sup>, Julio Aguirre<sup>a,1</sup>, Gonzalo Jiménez-Moreno<sup>a,2</sup>, Gerhard Schmiedl<sup>b,3</sup>, and Jorge Civis<sup>c,4</sup>

<sup>a</sup>Departamento de Estratigrafía y Paleontología, Facultad de Ciencias, Avenida Fuentenueva s.n., Universidad de Granada, 18002 Granada, Spain. (jnoel@ugr.es; jaguirre@ugr.es; gonzaloj@ugr.es).

<sup>b</sup>Center for Earth System Research and Sustainability, Bundesstraße 55, University of Hamburg, 20146 Hamburg, Germany. (gerhard.schmiedl@uni-hamburg.de).

<sup>c</sup>Instituto Geológico y Minero de España, Ríos Rosas 23, 28003 Madrid, Spain. (j.civis@igme.es).

\*Corresponding author: J. N. Pérez-Asensio, Departamento de Estratigrafía y Paleontología, Facultad de Ciencias, Avenida Fuentenueva s.n., Universidad de Granada, 18002 Granada, Spain. (jnoel@ugr.es). Tel.: +34 661086115

<sup>1</sup>Tel.: +34 958 248332

<sup>2</sup>Tel.: +34 958 248727

<sup>3</sup>Tel.: +49 40 42838 5008

<sup>4</sup>Tel.: +34 91 3495963

**Abstract**

The desiccation of the Mediterranean during the Messinian salinity crisis (MSC) is one of the most intriguing geological events of recent Earth history. However, the timing of its onset and end, as well as the mechanisms involved remain controversial. We present a novel approach to these questions by examining the MSC from the

Atlantic, but close to the Gibraltar Arc, analysing the complete Messinian record of the Montemayor-1 core of the Guadalquivir Basin (SW Spain). Flexural backstripping analysis shows a tectonic uplift trend that would have reduced the depth of the Rifian Corridors considerably. Nonetheless, the rate of tectonic uplift was insufficient to account for the close up of the corridors. At 5.97 Ma, a global cooling and associated glacioeustatic sea-level drop, estimated in 60 m, is observed. This would have been sufficient to restrict the Rifian corridors and to trigger the MSC. The later flooding of the Mediterranean occurred during a sea-level rise associated with global warming during a stable tectonic period. We postulate a two-step flooding event: 1) A glacioeustatic sea-level rise during interglacial stage TG 11 (5.52 Ma) led to subtropical Atlantic waters entering the west-central Mediterranean through pathways south of the Gibraltar Strait, probably the Rifian corridors. 2) A global sea-level drop at 5.4 Ma, that might have favoured intensification of regressive fluvial erosion in the Gibraltar threshold, along with the subsequent global sea-level rise would have generated the Gibraltar Strait leading to complete Mediterranean refilling during the earliest Pliocene.

*Keywords:* Messinian salinity crisis, glacioeustatic sea-level change, Messinian reflooding, backstripping, Guadalquivir Basin, SW Spain

## 1. Introduction

The Messinian salinity crisis (MSC) in the Mediterranean has attracted the interest of Earth scientists ever since the seminal publication by Hsü et al. (1973). The general consensus is that the Mediterranean was isolated from the Atlantic due to the closure of the Betic and the Rifian corridors and that this led to deposition of the Lower and Upper Evaporites. There are still key issues under intense debate. One of these concerns the main mechanisms that led to the isolation of the Mediterranean. Global glacioeustatic sea level lowering, regional tectonic uplift in the Gibraltar area, or a combination of both processes have been invoked as trigger mechanisms (Weijermars, 1988; Kastens, 1992; Aharon et al., 1993; Butler et al., 1999; Duggen et al., 2003; Hilgen et al., 2007). Additionally, there is no consensus on the timing and causes of the reestablishment of normal marine conditions in the Mediterranean at the end of the MSC (Martín and Braga, 1994; Riding et al., 1998; Krijgsman et al., 1999a; Hilgen et

al., 2007). These difficulties can largely be attributed to the complex Messinian paleogeography of the Mediterranean associated with a variety of local tectono-sedimentary regimes, and the continuing problems of accurate correlation of both deep-basin and marginal-basin deposits.

Here we present planktonic and benthic oxygen stable isotope data that, in combination with published information, could provide a solution to the MSC conundrum. We have studied the Montemayor-1 core (Guadalquivir Basin, SW Spain) (Fig. 1) that shows a continuous Messinian sedimentary record in the vicinity of the Gibraltar Arc. The core is accurately dated (Fig. 2) and provides an unbiased perspective of the MSC from the open Atlantic Ocean, offering the unique opportunity of linking global oceanic processes with regional Mediterranean events coeval with the desiccation. This could provide a comprehensive model for understanding the desiccation and re-filling of the Mediterranean during the Messinian. The establishment of this model is the main aim of this work.

## **2. The Montemayor-1 core**

The Montemayor-1 core is located close to Huelva (SW Spain) (37°16'N, 6°49'W; 52 m elevation) (Fig. 1) and consists of latest Tortonian-early Pliocene marine deposits (Larrasoña et al., 2008; Pérez-Asensio et al., 2012a). According to the age model established for the core by Pérez-Asensio et al. (2012b) and later supplemented by Jiménez-Moreno et al. (2013) the interval studied ranges from 6.17 to 5.19 Ma. This age model was developed using magnetobiostratigraphic (Larrasoña et al., 2008) and O stable isotope data (see a detailed explanation in Jiménez-Moreno et al., 2013) (Fig. 2). The age model shows that a discontinuity is present in the lower part of chron C3n and the uppermost part of chron C3r, and the core is continuous at least until the interglacial stage TG 7 (5.359 Ma). Therefore, the age model proves that most of the Messinian record is complete.

## **3. Methodology**

The stable oxygen isotope signals of foraminifers were used as a proxy of paleoclimatic changes related to glacioeustatic fluctuations (Figs. 3 and 4). The  $\delta^{18}\text{O}$

stable isotopes analysis were performed on about 10 individuals of *Cibicidoides pachydermus* for benthic foraminifera and 20 individuals of *Globigerina bulloides* for planktonic foraminifera which were picked from the size fraction >125 µm. Before the analyses, foraminiferal shells were cleaned with an ultrasonic cleaner, and washed with demineralised water. Isotope analyses were performed at the Leibniz-Laboratory for Radiometric Dating and Isotope Research in Kiel (Germany). In this work, all the results are presented in δ-notation (‰), and standardised to the Vienna Pee Dee belemnite (VPDB) scale. A certain value of the National Bureau of Standards (NBS) carbonate standard NBS-19 was used to define this scale (see Pérez-Asensio et al., 2012b for details).

Furthermore, the orbital obliquity and eccentricity were constructed using the Laskar orbital solutions La2004 and La2010 respectively (Laskar et al., 2004, 2011) following the recommendations of Laskar et al. (2011). To generate the ETP (eccentricity, obliquity, precession) curve the normalised eccentricity La2010 orbital solution, the normalised obliquity La2004 orbital solution and the negative normalised precession La2004 orbital solution were summed.

In addition, quantitative sea-level changes were estimated using a transfer function based on benthic foraminifera developed by Hohenegger (2005) and later modified by Báldi and Hohenegger (2008) and Hohenegger et al. (2008) (see a detailed explanation in Pérez-Asensio et al., 2012a).

Global sea-level curves of Hardenbol et al. (1998) and Miller et al. (2005), as well as the regional sea-level curve of 4th order eustatic cycles of Esteban et al. (1996) were used for comparison with the sea-level curve of the Montemayor-1 core.

Flexural backstripping analysis was carried out following the methodology proposed by Allen and Allen (1990). This method is used to reconstruct the vertical movement of the basin floor. Sediments are flexurally unloaded from the basement by applying different corrections for the paleobathymetric changes, compaction, loading effects of the sediments and eustatic sea-level fluctuations (Watts, 1988). According to the formula of Allen and Allen (1990), the vertical movement of the basement (Z) is:

$$Z = C[S[(\sigma_m - \sigma_s)/(\sigma_m - \sigma_w)] - \Delta Sli[(\sigma_w)/(\sigma_m - \sigma_w)]] + Wdi - \Delta Sli[(\sigma_m)/(\sigma_m - \sigma_w)]$$

where  $\sigma_m$  is mantle density ( $3,300 \text{ kg}\times\text{m}^{-3}$ ),  $\sigma_s$  is sediment density ( $1,400 \text{ kg}\times\text{m}^{-3}$ , average density for pelagic clay in marine environments (Hamilton, 1970; Orsi, 1991)),  $\sigma_w$  is water density ( $1,000 \text{ kg}\times\text{m}^{-3}$ ),  $W_{di}$  is paleobathymetry of the Montemayor-1 core estimated with the transfer function,  $\Delta S_{li}$  is the eustatic sea-level change derived from the curve of Miller et al. (2005),  $S$  is the original thickness before compaction, and  $\zeta$  is the isostatic compensation function.

The isostatic compensation function ( $\zeta$ ) was calculated with the following equation:

$$\zeta = [(\sigma_m - \sigma_s)] / [(\sigma_m - \sigma_s) + [D/g[(2\pi/\lambda)^4]]]$$

where  $g$  is gravitational acceleration ( $9.81 \text{ m}\times\text{s}^{-2}$ ),  $D$  is flexural rigidity ( $4.80 \times 10^{22} \text{ N}\times\text{m}$  for a effective elastic thickness ( $T_e$ ) of 20 km in the Betic Cordillera (van der Beek and Cloetingh, 1992)),  $\pi$  is the mathematical constant, and  $\lambda$  is the wavelength of the periodic load which is 90 km for the western sector of the Guadalquivir Basin.

The original thickness before compaction ( $S$ ) was estimated calculating the compaction of clays since the Montemayor-1 core consists of mostly bluish-greenish clays from the Arcillas de Gibrleón Formation (Fig. 2). For that purpose, the compaction of clays was calculated using the formula of Einsele (1992):

$$h_{sl} = [(1 - n_p)/(1 - n_l)] \times (h_{sp})$$

where  $h_{sl}$  is the original thickness before compaction,  $h_{sp}$  is the compacted thickness,  $n_l$  is the original mean porosity, and  $n_p$  is the final mean porosity after compaction. An average  $n_l$  of 80%, and  $n_p$  of 20% for clays was used (Leeder, 1982; Velde, 1996; Boggs, 2009). Using this formula, the compaction of the Montemayor-1 core is 75%.

#### 4. Results

The paleodepth curve derived from the transfer function based on benthic foraminifera shows a long-term decreasing trend with 3 significant sea-level drops (Fig. 3): 227 m at 5.98 Ma, 169 m at 5.76 Ma, and 97 m at 5.23 Ma.

The benthic oxygen isotope record has a fluctuating trend and shows a gradual increase from 6.17 to 5.79 Ma (TG 22) (Figs. 3 and 4). In this interval, the benthic  $\delta^{18}\text{O}$  values show an increase of 0.66‰ around 5.95 Ma, and another increase of 0.82‰ around 5.79 Ma (TG 22). Then,  $\delta^{18}\text{O}$  decreases and reaches average values around 0.5‰ from 5.7 Ma to 5.19 Ma. In this interval, a significant decrease of 0.68‰ is observed at 5.52 Ma (TG 11). The planktonic oxygen isotope record has a similar trend to the benthic O isotope record except for relatively low planktonic O values coinciding with high benthic O values around 5.79 Ma (TG 22). Furthermore, planktonic O values decrease by 1‰ at 5.52 Ma (TG 11), which is higher than the decrease of 0.68‰ observed in the benthic O isotope record (Fig. 4).

The flexural backstripping analysis shows a roughly stable tectonic period from 7.24 to 5.99 Ma (Fig. 5). In the interval from 5.99 to 5.76 Ma, there is an uplifting trend of 0.6 mm/yr. This trend is limited by two abrupt pulses of tectonic uplift with values of 18.7 mm/yr at 5.99 Ma and 16.5 mm/yr at 5.76 Ma. Another period with tectonic stability is observed from 5.76 to 5.38 Ma. Finally, there is a slight tectonic uplift from 5.38 to 5.22 Ma. In this interval, two significant uplifting pulses are found at 5.33 and 5.23 Ma.

## 5. Discussion

### 5.1. Onset of the MSC

The MSC started at  $5.97 \pm 0.02$  Ma (Krijgsman et al., 1999a; Manzi et al., 2013), coinciding with the onset of Lower Evaporite deposition. The paleodepth curve based on benthic foraminifera shows a significant sea-level fall of 227 m at this time based on benthic foraminifera (Pérez-Asensio et al., 2012a) (Fig. 3). A dramatic reduction in the dinoflagellate/pollen ratio in the core (Fig. 3) at this time also indicates shallowing (Jiménez-Moreno et al., 2013). Relative abundance of *Quercus* pollen, which mainly follows a long-term (400-ka) eccentricity trend (Jiménez-Moreno et al., 2013) (Fig. 3), and other thermophilous plants, decreased substantially at this time pointing to cool and arid conditions concurrent with the beginning of the MSC (Jiménez-Moreno et al., 2013). This cooling and sea-level drop match with minima of the ETP, eccentricity and obliquity orbital curves, as well as with an increase in the

benthic  $\delta^{18}\text{O}$  values of the Montemayor-1 core which is mainly forced by obliquity (Pérez-Asensio et al., 2012b) (Figs. 3 and 6). Similar increases in the benthic  $\delta^{18}\text{O}$  values associated with a sea-level lowering have been documented in the Atlantic and Pacific oceans (Shackleton et al., 1995, Shackleton and Hall, 1997; Vidal et al., 2002) (Fig. 4). All these evidences point to a glacioeustatic origin for the sea-level drop related to the onset of the MSC. This cooling was probably associated with ice-sheet expansions on western Antarctica and the Arctic taking place during the late Miocene (Zachos et al., 2001). Furthermore, it could be estimated quantitatively assuming the late Pleistocene  $\delta^{18}\text{O}$ /sea-level relationship, which relates an increase of 0.11‰ in the  $\delta^{18}\text{O}$  to a global sea-level fall of 10 m (Fairbanks and Matthews, 1978). According to this relationship, the benthic  $\delta^{18}\text{O}$  increase of 0.66‰ at the onset of the MSC would indicate a corresponding glacioeustatic sea-level fall of 60 m.

Flexural backstripping analysis shows a long-term tectonic stability period before the sea-level drop at the onset of the MSC. In addition, there is an uplifting trend from the MSC (5.99 Ma) to the TG 20 glacial stage (5.75 Ma) (Fig. 5). This time interval is limited by two pulses of tectonic rising with average values of 18.7 mm/yr at the base (5.99 Ma) and 16.5 mm/yr at the top (5.76 Ma). They are extremely high and probably unusually exaggerated due to the small global sea-level changes used in the analysis (Miller et al., 2005), which indicate corresponding sea-level drops of 40 m and 16.8 m. However, our paleobathymetric data show sea-level falls of 227 m and 169 m respectively (Pérez-Asensio et al., 2012a). Furthermore, these estimated sea-level drops based on benthic foraminifera could also be exaggerated. Consequently, the high difference between the estimated sea-level drops and coeval global sea-level falls results in an anomalously high tectonic uplift rates. Therefore, the tectonic uplifting pulses at 5.99 and 5.76 Ma appear not reliable. Considering these two pulses as outliers, the resulting average uplifting rate is 0.6 mm/yr, well within the ranges estimated for the Late Neogene uplift of the Betic Cordillera: from 0.2 to 0.7 mm/yr (Weijermars et al., 1985; Braga et al., 2003). The onset of the MSC was at  $5.97 \pm 0.02$  Ma which covers an interval of 0.04 Ma. The tectonic uplift of 0.6 mm/yr or 600 m/Ma would have produced a sea-level drop of 24 m during this interval.

Prior to the MSC, maximum paleodepths for the Betic and Rifian corridors were about 120 m and 100 m, respectively (Martín et al., 2001; Krijgsman et al., 1999b). The last Betic seaway, the Guadalhorce Corridor, was closed at 6.18 Ma (Pérez-Asensio et



al., 2012b). Since this event, the Rifian Corridors remained as the only Atlantic-Mediterranean gateway (Esteban et al., 1996). The estimated long-term tectonic trend of 0.6 mm/yr produced by the collision of the African and Eurasian plates would have reduced the depth of the Rifian Corridors substantially. Some estimates even suggest that the depth of the corridors might have been around 50 m prior to the MSC (Rohling et al., 2008). With this shallow corridor, small variations in sea-level could result in gypsum saturation in the Mediterranean (Rohling et al., 2008; Meijer, 2012). Nonetheless, the sea-level drop of 24 m produced by tectonic uplift at the onset of MSC was insufficient to close up this 50 m deep corridor. In contrast, the estimated glacioeustatic sea-level fall of 60 m at 5.97 Ma would be sufficient to restrict the Rifian corridors and produce a sufficiently negative water budget in the Mediterranean triggering the MSC. In summary, tectonic uplift was a secondary controlling factor, and the MSC was primarily triggered by a glacioeustatic sea-level fall.

## 5.2. *Closing the MSC*

It has been suggested that the Upper Evaporites deposition took place from 5.50 Ma to 5.33 Ma (Miocene/Pliocene boundary) (Krijgsman et al., 1999a). These deposits have been assumed coeval with the brackish-freshwater Lago-Mare deposits, implying a partial or complete disconnection of the Mediterranean (Krijgsman et al., 1999a). The presence of brackish-fresh waters in the whole Mediterranean during the late Miocene contrasts with the necessity of a continuous Atlantic marine inflow along with blocked Mediterranean outflow in order to produce kilometre-thick evaporites (Meijer and Krijgsman, 2005; Meijer, 2006; Krijgsman and Meijer, 2008). This has been also proven by geochemical data that suggest a marine origin for the Upper Evaporites in the Sorbas and Níjar basins (Playà et al., 1997; Lu et al., 2001, 2002). Moreover, fully marine post-evaporitic sediments were deposited in marginal basins of SE Spain during the late Messinian as consequence of a sea-level rise during the late Messinian (Riding et al., 1998; Aguirre and Sánchez-Almazo, 2004; Braga et al., 2006). These deposits contain a plethora of fully marine fauna, including hermatypic corals, coralline algae, echinoderms, demosponges, fish, bryozoans, foraminifera and bivalves, that inhabited the western and central Mediterranean during the late Messinian (Hsü et al., 1977, 1978; Cita et al., 1978; Riding et al., 1991; Martín et al., 1993; Martín and Braga, 1994;

Comas et al., 1996, Riding et al., 1998; Aguirre and Sánchez-Almazo, 2004; Braga et al., 2006, Carnevale et al., 2006a, 2006b, 2008; Bourillot et al., 2010a, 2010b).

In the central Mediterranean, the late Messinian transgression is also well-documented by different geochemical proxies including strontium, carbon and oxygen isotopes, and fish assemblages (Keogh and Butler, 1999; Carnevale et al., 2008). Furthermore, geomorphologic features of late Messinian drainage systems in the western Mediterranean also point to a flooding before the Miocene/Pliocene boundary (Estrada et al., 2011; García et al., 2011, Bache et al., 2012). To accommodate all these findings, we postulate a two-step reflooding process of the Mediterranean during the latest Messinian.

Our results reveal a shift of 1‰ and 0.7‰ in  $\delta^{18}\text{O}$  of planktonic and benthic foraminifera, respectively, from the glacial stage TG 12 (5.55 Ma) to the interglacial TG 11 (5.52 Ma) that correlates with a global sea level rise (Figs. 3 and 4). Eccentricity and ETP curves increase supporting a glacioeustatic control of this isotopic shift (Fig. 3). The same trend is recorded in the Rifian Corridors, Atlantic and Pacific oceans (Shackleton et al., 1995; Vidal et al., 2002; van der Laan et al., 2006) (Fig. 4), and is related to a period of global warming that persisted until the mid Pliocene (Vidal et al., 2002). Using the  $\delta^{18}\text{O}$ /sea-level relationship of Fairbanks and Matthews (1978) for the late Pleistocene, the decrease of 0.7‰ in benthic  $\delta^{18}\text{O}$  corresponds to a sea-level rise of 63.6 m, close to our estimation of 68.3 m with the transfer function based on benthic foraminifera (Pérez-Asensio et al., 2012a). A similar sea-level rise of 70 m is observed in the marginal basins of SE Spain (Bourillot et al., 2010a). In addition, global sea level rise during the TG 12-TG 11 transition is ~75 m (Miller et al., 2005) (Fig. 4).

Backstripping analysis shows a tectonic stable period during the late Messinian (Fig. 5), suggesting that tectonism in the vicinity of the Gibraltar Arc was insignificant. Therefore, we propose that the glacioeustatic sea level rise at TG 11 (5.52 Ma) could have triggered the first reflooding step of the western and central Mediterranean shortly before the Miocene/Pliocene boundary (Fig. 6). This agrees with the view that a small connection to the Atlantic was sufficient to quickly reinundate the Mediterranean (Meijer and Krijgsman, 2005). This conclusion is also corroborated by the presence of late Messinian marine deposits in western and central Mediterranean marginal basins (Martín and Braga, 1994; Riding et al., 1998; Braga et al., 2006; Carnevale et al., 2006a, 2006b, 2008; Bourillot et al., 2010a, 2010b).

It is generally assumed that Atlantic waters flooded into the Mediterranean through the Gibraltar Strait (Blanc, 2002; Meijer and Krijgsman, 2005; Estrada et al., 2011; Bache et al., 2012). In such a case, cold Atlantic waters would enter the Mediterranean (Martín et al., 2010). However, photozoan carbonates developed at the uppermost Messinian deposits in SE Spain (Martín and Braga, 1994; Braga et al., 2006; Martín et al., 2010). These data indicate the inflow of warm subtropical Atlantic waters into the Mediterranean during the first reflooding step from areas south of the Gibraltar Strait, probably through Rifian Corridors, promoting the formation of coral reefs in SE Spain (Martín et al., 2010). Messinian canyons excavated at NW Morocco shelf might have accounted for this first inundation (Loget and van den Driessche, 2006). Furthermore, the Rifian Corridors were not completely closed during the MSC because a continuous inflow of Atlantic water is crucial to develop kilometre-thick evaporite deposits formed in the Mediterranean basin during the MSC (Meijer and Krijgsman, 2005; Meijer, 2006; Krijgsman and Meijer, 2008). Hence, a reflooding via the Rifian Corridors during the global sea-level rise related to TG 11 is very likely.

In the Sorbas Basin (SE Spain), marine post-evaporitic deposits are overlain by continental sediments of the Zorreras Member (Martín and Braga, 1994; Martín-Suárez et al., 2000). This indicates a sea-level drop at the very end of the Messinian (Martín and Braga, 1994; Martín and Braga, 1996). Bourillot et al. (2010a) estimated a sea-level fall of 30-40 m at the end of the Terminal Carbonate Complex (latest Messinian) in SE Spain basins. This, in turn, coincides with a global sea-level fall of approximately 25 m at about 5.4 Ma (TG 8) (Miller et al., 2005) (Fig. 3). In the central Mediterranean (Sicily, S Italy), this sea-level drop is related to the deposition of the non-marine fluvio-lacustrine siliciclastic Arenazzolo formation (Hilgen and Langereis, 1988; van Couvering et al., 2000).

In the second step of the Mediterranean reflooding, the sea-level fall at 5.4 Ma would have accelerated the regressive fluvial erosion in the Gibraltar Isthmus (Blanc, 2002; Loget et al., 2005; Loget and van den Driessche, 2006). The combined effect of local regressive erosion of the Gibraltar threshold in a context of global sea-level rising that started at 5.52 Ma and continued during the early Pliocene (Vidal et al., 2002), finally led to the complete opening of the Gibraltar Strait during the earliest Zanclean. As a consequence of the final opening of the Gibraltar Strait, catastrophic flows of more northern-derived and cooler Atlantic waters flooded the Mediterranean Sea (Martín et

al., 2010), resulting in a steady rise of the Mediterranean sea-level and filling up the entire Mediterranean Basin.

Bourillot et al. (2010a) proposed a similar two-step reflooding model. Nevertheless, this model contrasts with our proposal since Bourillot et al. (2010a) stated that the Atlantic waters flow into the Mediterranean through the Betic and/or Rifian corridors. Pérez-Asensio et al. (2012b) have recently demonstrated that the last active Betic seaway, the Guadalhorce Corridor, was closed at 6.18 Ma. Therefore, the first step of the reflooding should have been through the Rifian Corridors. This is supported by the inferred entrance of warm Atlantic waters, which is required to foster the development of coral reefs in the western Mediterranean.

Bache et al. (2009, 2012) also suggested that the entire Mediterranean was reflooded through the Strait of Gibraltar in two steps during interglacial TG 11 (late Messinian). According to these authors, during the step I (5.56?–5.46 Ma), there was a relatively moderate and slow sea-level rise as a result of the beginning of a progressively increasing erosion of the Gibraltar isthmus. Then, during the step II (5.46 Ma), a particularly sudden and dramatic flooding was produced by the collapse of the Gibraltar channel. However, as suggested above, the reflooding related to the interglacial TG 11 was most likely through the Rifian Corridors as indicated by the presence of coral reefs in the western Mediterranean during the late Messinian. Moreover, this model postulates that the entire Mediterranean was flooded at 5.46 Ma. This means that Bache et al. (2009, 2012) did not take into consideration the relative sea-level drop shortly before the early Pliocene that promoted continental deposition in the western (Zorerras Member in the Sorbas Basin) and central Mediterranean (the Arenazzolo Formation of Sicily). Thus, the second step of the reflooding must have occurred during the earliest Zanclean, and not during the late Messinian, when the ultimate opening of the Strait of Gibraltar took place. Therefore, timing and reflooding pathways proposed by Bache et al. (2009, 2012) for the two-step re-filling of the Mediterranean are improbable since they are not concurrent with the available evidence.

## 6. Conclusions

Our results show that tectonics in the Gibraltar Arc area played a secondary role in the onset of the MSC, and it had no influence in the end of the MSC. A glacioeustatic

sea-level drop of at least 60 m was the triggering mechanism of the MSC initiation. For the end of the MSC, we postulate a two-steps flooding of the Mediterranean: 1) warm meridional Atlantic waters entering western-central Mediterranean through Rifian Corridors during the glacioeustatic stage TG 11 (5.52 Ma), and 2) intensification of regressive fluvial erosion in the Gibraltar threshold, together with a global sea-level rise, led to the opening of the Gibraltar Strait during the earliest Pliocene and the complete refilling of the Mediterranean.

### Acknowledgments

We thank one anonymous reviewer and the editor Dr. Thomas M. Cronin for their comments and suggestions which have been very valuable to improve the quality of the paper. This work is part of the projects CGL2010-20857 and CGL2009-11539, and the Research Group RNM-190. JNPA was funded by a F.P.U. grant (ref. AP2007-00345). We acknowledge Dr. Kotthoff for his comments on an early draft. We also thank N. Andersen (Leibniz-Laboratory, Kiel, Germany) for stable isotope analyses.

### References:

- Aguirre, J., Sánchez-Almazo, I.M., 2004. The Messinian post-evaporitic deposits of the Gafares area (Almería-Níjar basin, SE Spain). A new view of the “Lago-Mare” facies. *Sediment. Geol.* 168, 71–95.
- Aharon, P., Goldstein, S.L., Wheeler, C.W., Jacobson, G., 1993. Sea-level events in the South Pacific linked with the Messinian salinity crisis. *Geology* 21, 771–775.
- Allen, P.A. Allen, J.R., 1990. *Basin analysis. Principles and Applications*. Blackwell Scientific Publications, Oxford.
- Bache, F., Olivet, J.L., Gorini, C., Rabineau, M., Baztan, J., Aslanian, D., Suc, J.-P., 2009. Messinian erosional and salinity crises: view from the Provence Basin (Gulf of Lions, Western Mediterranean). *Earth Planet. Sc. Lett.* 286, 139–157.

- Bache, F., Popescu, S.-M., Rabineau, M., Gorini, C., Suc, J.-P., Clauzon, G., Olivet, J.-L., Rubino, J.-L., Melinte-Dobrinescu, M.C., Estrada, F., Londeix, L., Armijo, R., Meyer, B., Jolivet, L., Jouannic, G., Leroux, E., Aslanian, D., Dos Reis, A.T., Mocochain, L., Dumurdžanov, N., Zagorchev, I., Lesić, V., Tomić, D., Çağatay, M.N., Brun, J.-P., Sokoutis, D., Csato, I., Uçarkus, G., Çakir, Z., 2012. A two-step process for the reflooding of the Mediterranean after the Messinian Salinity Crisis. *Basin Res.* 24, 125–153.
- Báldi, K., Hohenegger, J., 2008. Paleoecology of benthic foraminífera of Baden-Sooss section (Badenian, Middle Miocene, Vienna Basin, Austria). *Geol. Carpath.* 59, 411–424.
- Blanc, P.-L., 2002. The opening of the of the Plio-Quaternary Gibraltar Strait: assessing the size of a cataclysm. *Geodin. Acta* 15, 303–317.
- Boggs, S., 2009. *Petrology of Sedimentary Rocks*. Cambridge University Press, Cambridge.
- Bourillot, R., Vennin, E., Rouchy, J.M., Blanc-Valleron, M.M., Caruso, A., Durllet, C., 2010a. The end of the Messinian Salinity Crisis in the western Mediterranean: insights from the carbonate platforms of south-eastern Spain. *Sediment. Geol.* 229, 224–253.
- Bourillot, R., Vennin, E., Rouchy, J.M., Durllet, C., Rommevaux, V., Kolodka, C., Knap, F., 2010b. Structure and evolution of a Messinian mixed carbonate-siliciclastic platform: the role of evaporites (Sorbas Basin, South-east Spain). *Sedimentology* 57, 477–512.
- Braga, J.C., Martín, J.M., Quesada, C., 2003. Patterns and average rates of late Neogene–Recent uplift of the Betic Cordillera, SE Spain. *Geomorphology* 50, 3–26.

- Braga, J.C., Martín, J.M., Riding, R., Aguirre, J., Sánchez-Almazo, I.M., Dinarès-Turell, J., 2006. Testing models for the Messinian salinity crisis: the Messinian record in Almería, SE Spain. *Sediment. Geol.* 188–189, 131–154.
- Butler, R.W.H., McClelland, E., Jones, R.E., 1999. Calibrating the duration and timing of the Messinian salinity crisis in the Mediterranean: linked tectonoclimatic signals in thrust-top basins of Sicily. *J. Geol. Soc. London* 156, 827–835.
- Carnevale, G., Caputo, D., Landini, W., 2006a. Late Miocene fish otoliths from the Colombacci Formation (Northern Apennines, Italy): implications for the Messinian ‘Lago-mare’ event. *Geol. J.* 41, 537–555.
- Carnevale, G., Landini, W., Sarti, G., 2006b. Mare versus Lago-mare: marine fishes and the Mediterranean environment at the end of the Messinian salinity crisis. *J. Geol. Soc. London* 163, 75–80.
- Carnevale, G., Longinelli, A., Caputo, D., Barbieri, M., Landini, W., 2008. Did the Mediterranean marine reflooding precede the Mio-Pliocene boundary? Paleontological and geochemical evidence from upper Messinian sequences of Tuscany, Italy. *Palaeogeogr. Palaeoclimatol. Palaeoecol.* 257, 81–105.
- Cita, M.B., Wright, R.C., Ryan, W.B.F., Longinelli, A., 1978. Messinian paleoenvironments. *Initial Rep. Deep Sea Drill. Proj.* 42A, 1003–1035.
- Comas, M.C., Zahn, R., Klaus, A. et al., 1996. Proceedings of the Deep Sea Drilling Project, Init. Rept. 161. U.S. Government Printing Office, Washington, D.C., 1023 pp.
- Duggen, S., Hoernle, K., van den Bogaard, P., Rüpke, L. Morgan, J.P., 2003. Deep roots of the Messinian salinity crisis. *Nature* 422, 602–606.
- Einsele, G., 1992. *Sedimentary Basins, Evolution, Facies and Sediment Budget*. Springer-Verlag, Berlin.

- Esteban, M., Braga, J.C., Martín, J.M., Santisteban, C., 1996. Western Mediterranean reef complexes. In: Franseen, E.K., Esteban, M., Ward, W.C., Rouchy, J.M. (Eds.), Models for Carbonate Stratigraphy from Miocene Reef Complexes of Mediterranean Regions. : Concepts in Sedimentology and Paleontology, Vol. 5. Society of Economic Paleontologists and Mineralogists, Tulsa, Oklahoma, pp. 55–72.
- Estrada, F., Ercilla, G., Gorini, C., Alonso, B., Vázquez, J.T., García-Castellanos, D., Juan, C., Maldonado, A., Ammar, A., Elabbassi, M., 2011. Impact of pulsed Atlantic water inflow into the Alboran Basin at the time of the Zanclean flooding. *Geo-Mar. Lett.* 31, 361–376.
- Fairbanks, R.G., Matthews, R.K., 1978. The Marine Oxygen Isotope Record in Pleistocene Coral, Barbados, West Indies. *Quaternary Res.* 10, 181–196.
- García, M., Maillard, A., Aslanian, D., Rabineau, M., Alonso, B., Gorini, C., Estrada, F., 2011. The Catalan margin during the Messinian Salinity Crisis: physiography, morphology and sedimentary record. *Mar. Geol.* 284, 158–174.
- Hamilton, E.L., 1970. Sound Velocity and Related Properties of Marine Sediments, North Pacific. *J. Geophys. Res.* 75, 4423–4446.
- Hardenbol, J., Thierry, J., Farley, M.B., Jaquin, T., de Graciansky, P., Vail, P.R., 1998. Mesozoic and Cenozoic sequence chronostratigraphic framework of European basins - chart 2: Cenozoic sequence chronostratigraphy. In: de Graciansky, P., Hardenbol, J., Jaquin, T., Vail, P.R. (Eds.), Mesozoic and cenozoic sequence stratigraphy of european basins: SEPM Special Publication, 60.
- Hilgen, F.J., Langereis, C.G. 1988. The age of the Miocene-Pliocene boundary in the Capo-Rossello area (Sicily). *Earth Planet. Sc. Lett.* 9, 214–222.



- Hilgen, F., Kuiper, K., Krijgsman, W., Snel, E., van der Laan, E., 2007. Astronomical tuning as the basis for high resolution chronostratigraphy: the intricate history of the Messinian Salinity Crisis. *Stratigraphy* 4, 231–238.
- Hohenegger, J., 2005. Estimation of environmental paleogradient values based on presence/absence data: a case study using benthic foraminifera for paleodepth estimation. *Palaeogeogr. Palaeoclimatol. Palaeoecol.* 217, 115–130.
- Hohenegger, J., Andersen, N., Báldi, K., Ćorić, S., Pervesler, P., Rupp, C., Wagreich, M., 2008. Paleoenvironment of the Early Badenian (Middle Miocene) in the southern Vienna Basin (Austria) — multivariate analysis of the Baden-Sooss section. *Geol. Carpath.* 59, 461–487.
- Hsü, K.J., Ryan, W.B.F., Cita, M.B., 1973. Late Miocene Desiccation of the Mediterranean. *Nature* 242, 240–244.
- Hsü, K.J., Montadert, L., Bernoulli, D., Cita, M.B., Erickson, A., Garrison, R.E., Kidd, R.B., Mèlierés, F., Müller, C., Wright, R., 1977. History of the Messinian salinity crisis. *Nature* 267, 399–403.
- Hsü, K.J., Montadert, L., et al., 1978. Initial Reports of the Deep Sea Drilling Project. U.S. Government Printing Office, Washington, D.C., 42A, 1249 pp.
- Jiménez-Moreno, G., Pérez-Asensio, J.N., Larrasoana, J.C., Aguirre, J., Civis, J., Rivas-Carballo, M.R., Valle-Hernández, M.F., González-Delgado, J.A., 2013. Vegetation, sea-level and climate changes during the Messinian salinity crisis. *Geol. Soc. Am. Bull.* 125, 432–444.
- Kastens, K.A., 1992. Did a glacio-eustatic sea level drop trigger the Messinian Salinity crisis? New evidence from Ocean Drilling Program site 654 in the Tyrrhenian Sea. *Paleoceanography* 7, 333–356.

- Keogh, S.M., Butler, R.W.H., 1999. The Mediterranean water body in the late Messinian: interpreting the record from the marginal basins in Sicily. *J. Geol. Soc. London* 156, 837–846.
- Krijgsman, W., Meijer, P.Th., 2008. Depositional environments of the Mediterranean “Lower Evaporites” of the Messinian salinity crisis: Constraints from quantitative analyses. *Mar. Geol.* 253, 73–81.
- Krijgsman, W., Hilgen, F.J., Raffi, I., Sierro, F.J., Wilson, D.S., 1999a. Chronology, causes and progression of the Messinian salinity crisis. *Nature* 400, 652–655.
- Krijgsman, W., Langereis, C.G., Zachariasse, W.J., Boccaletti, M., Moratti, G., Gelati, R., Iaccarino, S., Papani, G., Villa, G., 1999b. Late Neogene evolution of the Taza-Guercif Basin (Rifian Corridor, Morocco) and implications for the Messinian salinity crisis. *Mar. Geol.* 153, 147–160.
- Larrasoana, J.C., González-Delgado, J.A., Civis, J., Sierro, F.J., Alonso-Gavilán, G., Pais, J., 2008. Magnetobiostratigraphic dating and environmental magnetism of Late Neogene marine sediments recovered at the Huelva-1 and Montemayor-1 boreholes (lower Guadalquivir basin, Spain). *Geo-Temas* 10, 1175–1178.
- Laskar, J., Robutel, P., Joutel, F., Gastineau, M., Correia, A.C.M., Levrard, B., 2004. A long-term numerical solution for the insolation quantities of the Earth. *Astron. Astrophys.* 428, 261–285.
- Laskar, J., Fenga, A., Gastineau, M., Manche, H., 2011. La2010: a new orbital solution for the long-term motion of the Earth. *Astron. Astrophys.* 532, A89. doi: 10.1051/0004-6361/201116836.
- Leeder, M.R., 1982. *Sedimentology, Processes and Products*. Allen and Unwin, London.
- Loget, N., van den Driessche, J., 2006. On the origin of the Strait of Gibraltar: *Sediment. Geol.* 188-189, 341–356.

- Loget, N., van den Driessche, J., Davy, P., 2005. How did the Messinian Salinity Crisis end?. *Terra Nova* 17, 414–419.
- Lu, F.H., Meyers, W.J., Schoonen, M.A., 2001. S and O (SO<sub>4</sub>) isotopes, simultaneous modelling, and environmental significance of the Nijar Messinian gypsum, Spain. *Geochim. Cosmochim. Ac.* 65, 30811–33092.
- Lu, F.H., Meyers, W.J., Hanson, G.N., 2002. Trace elements and environmental significance of Messinian gypsum deposits, the Nijar basin, southeastern Spain. *Chem. Geol.* 192, 149– 161.
- Manzi, V., Gennari, R., Hilgen, F., Krijgsman, W., Lugli, S., Roveri, M., Sierro, F.J., 2013. Age refinement of the Messinian salinity crisis onset in the Mediterranean. *Terra Nova*, 0, 1–8, doi: 10.1111/ter.12038.
- Martín, J.M., Braga, J.C., 1994. Messinian events in the Sorbas basin in southeastern Spain and their implications in the recent history of the Mediterranean. *Sediment. Geol.* 90, 257–268.
- Martín, J.M., Braga, J.C., 1996. Tectonic signals in the Messinian stratigraphy of the Sorbas basin (Almería, SE Spain). In: Friend, P.F., Dabrio, C.J. (Eds.), *Tertiary Basins of Spain: The Stratigraphic Record of Crustal Kinematics*. World and Regional Geology Series, vol. 6. Cambridge Univ. Press, Cambridge, pp. 387– 391.
- Martín, J.M., Braga, J.C., Riding, R., 1993. Siliciclastic stromatolites and thrombolites, Late Miocene, S.E. Spain. *J. Sediment. Res.* 63, 131–139.
- Martín, J.M., Braga, J.C., Betzler, C., 2001. The Messinian Guadalhorce corridor: the last northern, Atlantic–Mediterranean gateway. *Terra Nova* 13, 418–424.
- Martín, J.M., Braga, J.C., Aguirre, J., Puga-Bernabéu, A., 2009. History and evolution of the North-Betic Strait (Prebetic Zone, Betic Cordillera): a narrow, early Tortonian,

- tidal-dominated, Atlantic–Mediterranean marine passage. *Sediment. Geol.* 216, 80–90.
- Martín, J.M., Braga, J.C., Sánchez-Almazo, I.M., Aguirre, J., 2010. Temperate and tropical carbonate-sedimentation episodes in the Neogene Betic basins (S Spain) linked to climatic oscillations and changes in the Atlantic-Mediterranean connections. Constraints with isotopic data. In: Mutti, M., Piller, W., Betzler, C. (Eds.), *Carbonate systems during the Oligocene–Miocene climatic transition* : International Association of Sedimentologists Special Publication, No. 42. Blackwell, Oxford, pp. 49–69.
- Martín-Suárez, E., Freudenthal, M., Krijgsman, W., Ritger Fortuin, A., 2000. On the age of the continental deposits of the Zorerras Member (Sorbas basin, SE Spain). *Geobios* 33, 505–512.
- Meijer, P.Th., 2006. A box model of the blocked-outflow scenario for the Messinian Salinity Crisis. *Earth Planet. Sc. Lett.* 248, 486–494.
- Meijer, P.Th., 2012. Hydraulic theory of sea straits applied to the onset of the Messinian Salinity Crisis. *Mar. Geol.* 326–328, 131–139.
- Meijer, P.Th., Krijgsman, W., 2005. A quantitative analysis of the desiccation and re-filling of the Mediterranean during the Messinian Salinity Crisis. *Earth Planet. Sc. Lett.* 240, 510–520.
- Miller, K.G., Kominz, M.A., Browning, J.V., Wright, J.D., Mountain, G.S., Katz, M.E., Sugarman, P.J., Cramer, B.S., Christie-Blick, N., Pekar, S.F., 2005. The Phanerozoic record of global sea-level change. *Science* 310, 1293–1298.
- Orsi, T.H., 1991. Equations for estimating sound velocity and velocity ratio of marine sediments: Brazil Basin (NW South Atlantic). *J. Acoust. Soc. Am.* 90, 2851–2853.

- Pérez-Asensio, J.N., Aguirre, J., Schmiedl, G., Civis, J., 2012a. Messinian paleoenvironmental evolution in the lower Guadalquivir Basin (SW Spain) based on benthic foraminifera. *Palaeogeogr. Palaeoclimatol. Palaeoecol.* 326–328, 135–151.
- Pérez-Asensio, J.N., Aguirre, J., Schmiedl, G., Civis, J., 2012b. Impact of restriction of the Atlantic-Mediterranean gateway on the Mediterranean Outflow Water and eastern Atlantic circulation during the Messinian. *Paleoceanography* 27, PA3222, doi:10.1029/2012PA002309.
- Playà, E., Rosell, L., Ortí, F., 1997. Geoquímica isotópica ( $\delta^{34}\text{S}$ ,  $^{87}\text{Sr}/^{86}\text{Sr}$ ) y contenidos en estroncio de las evaporitas messinienses de la cuenca de Sorbas (Almería). In: Calvo, J.P., Morales, J. (Eds.), *Avances en el Conocimiento del Terciario Ibérico*. Universidad Complutense de Madrid-Museo Nacional de Ciencias Naturales, Madrid, pp. 161–164.
- Riding, R., Martín, J.M., Braga, J.C., 1991. Coral–stromatolite reef framework, Upper Miocene, Almería, Spain. *Sedimentology* 38, 799–818.
- Riding, R., Braga, J.C., Martín, J.M., Sánchez-Almazo, I.M., 1998. Mediterranean Messinian salinity crisis: constraints from a coeval marginal basin, Sorbas, southeastern Spain. *Mar. Geol.* 146, 1–20.
- Rohling, E.J., Schiebel, R., Siddall, M., 2008. Controls on Messinian Lower Evaporite cycles in the Mediterranean. *Earth Planet. Sc. Lett.* 275, 165–171.
- Shackleton, N. J., Hall, M. A., 1997. The late Miocene stable isotope record, Site 926. *Proceedings of the Ocean Drilling Program, Scientific Results* 154, 367–374.
- Shackleton, N.J., Hall, M.A., Pate, D., 1995. Pliocene stable isotope stratigraphy of site 846. *Proceedings of the Ocean Drilling Program, Scientific Results* 138, 337–355.
- van Couvering, J.A., Castradori, D., Cita, M.B., Hilgen, F.J., Rio, D., 2000. The base of the Zanclean Stage and of the Pliocene Series. *Episodes* 23 (3), 179–187.

- van der Beek, P.A., Cloetingh, S., 1992. Lithospheric flexure and the tectonic evolution of the Betic Cordilleras (SE Spain). *Tectonophysics* 203, 325-344.
- van der Laan, E., Gaboardi, S., Hilgen, F.J., Lourens, L.J., 2005. Regional climate and glacial control on high-resolution oxygen isotope records from Ain El Beida (latest Miocene, NW Morocco): A cyclostratigraphic analysis in the depth and time domain. *Paleoceanography* 20, PA1001. doi: 10.1029/2003PA000995.
- van der Laan, E., Snel, E., de Kaenel, E., Hilgen, F.J., Krijgsman, W., 2006. No major deglaciation across the Miocene-Pliocene boundary: integrated stratigraphy and astronomical tuning of the Loulja sections (Bou Regreg area, NW Morocco). *Paleoceanography* 21, PA3011. doi:10.1029/2005PA001193.
- Velde, B., 1996. Compaction trends of clay-rich deep sea sediments. *Mar. Geol.* 133, 193–201.
- Vidal, L., Bickert, T., Wefer, G., Röhl, U., 2002. Late Miocene stable isotope stratigraphy of SE Atlantic ODP Site 1085: Relation to Messinian events. *Mar. Geol.* 180, 71–85.
- Watts, A.B., 1988. Gravity anomalies, crustal structure and flexure of the lithosphere at the Baltimore Canyon Trough. *Earth and Planetary Science Letters* 89, 221–238.
- Weijermars, R., 1988. Neogene tectonics in the Western Mediterranean may have caused the Messinian Salinity Crisis and an associated glacial event. *Tectonophysics* 148, 211–219.
- Weijermars, R., Roep, T.B., van den Eeckhout, B., Postma, G., Kleverlaan, K., 1985. Uplift history of a Betic fold nappe inferred from Neogene–Quaternary sedimentation and tectonics (in the Sierra Alhamilla and Almeria, Sorbas and Tabernas Basins of the Betic Cordilleras, SE Spain). *Geol. Mijnbouw* 64, 397–411.

Zachos, J.C., Pagani, M., Sloan, L., Thomas, E., Billups, K., 2001. Trends, Rhythms, and Aberrations in Global Climate 65 Ma to Present. *Science* 292, 686–693.

ACCEPTED MANUSCRIPT

## Figure captions

**Figure 1.** Paleogeographic map of the Gibraltar Arc area during the early Messinian, when the last active Betic gateway, the Guadalhorce Corridor, was open (based on Martín et al., 2009). The asterisk indicates the location of the studied core.

**Figure 2.** Age model and sedimentation rate (in cm/kyr) for the Montemayor-1 core (based on Pérez-Asensio et al., 2012b and Jiménez-Moreno et al., 2013). Position of glacial stages TG 22, and TG 12, and interglacial stage TG 7 is indicated. Question marks show imprecision in the age model.

**Figure 3.** A: Relative abundance of *Quercus* pollen (Jiménez-Moreno et al., 2013). B: Dinocyst/pollen ratio (Jiménez-Moreno et al., 2013) C: Paleodepth estimate based on benthic foraminiferal assemblages (Pérez-Asensio et al., 2012a). D: Eccentricity curve from La2010 orbital solution (Laskar et al., 2011). E: Obliquity curve from La2004 orbital solution (Laskar et al., 2004). F: Eccentricity, tilt and precession (ETP) curve. G: Benthic  $\delta^{18}\text{O}$  record in ‰ VPDB from the Montemayor-1 core. H: Global sea-level curves of Hardenbol et al. (1998) (light grey shading) and Miller et al. (2005) (black line), as well as the 4th order eustatic cycles of Esteban et al. (1996) (dark grey shading). Ages of the MSC onset ( $5.97 \pm 0.02$  Ma) and termination (5.52 Ma) are indicated with vertical lines.

**Figure 4.** A: Benthic foraminiferal O isotope record from Site 926 in the Atlantic Ocean (Shackleton and Hall, 1997). B: Benthic foraminiferal O isotope record from Site 1085 in the Atlantic Ocean (Vidal et al., 2002). C: Benthic foraminiferal O isotope record



from Site 846 in the Pacific Ocean (Shackleton et al., 1995). D: Global sea-level curve (Miller et al., 2005). E: Planktonic (grey) foraminiferal O isotope record from the Montemayor-1 core. F: Benthic (black) foraminiferal O isotope record from the Montemayor-1 core. Results are presented in ‰ VPDB. Age of the MSC onset and termination are indicated by the vertical lines.

**Figure 5.** Estimation of the vertical movement of the basement in meters obtained by flexural backstripping analysis. Main stable tectonic periods, uplift trends, onset and end of the MSC are shown.

**Figure 6.** Benthic oxygen isotope record (black) in ‰ VPDB from the Montemayor-1 and obliquity curve (grey) from La2004 orbital solution *versus* age (based on Jiménez-Moreno et al., 2013). Glacial and interglacial TG stages follow the nomenclature of Shackleton et al. (1995) and van der Laan et al. (2005, 2006). Horizontal dashed lines mark the ages of the onset and the termination of the MSC. The Miocene-Pliocene boundary is indicated by a horizontal solid line.

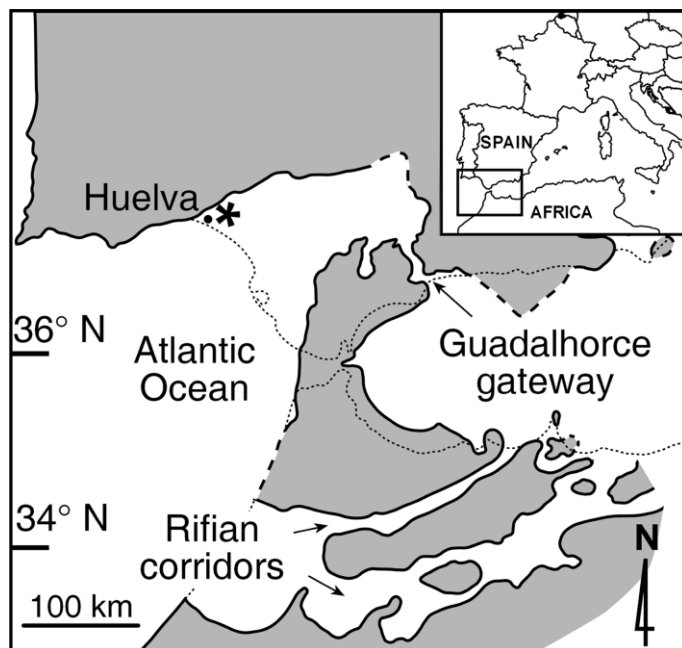


Figure 1

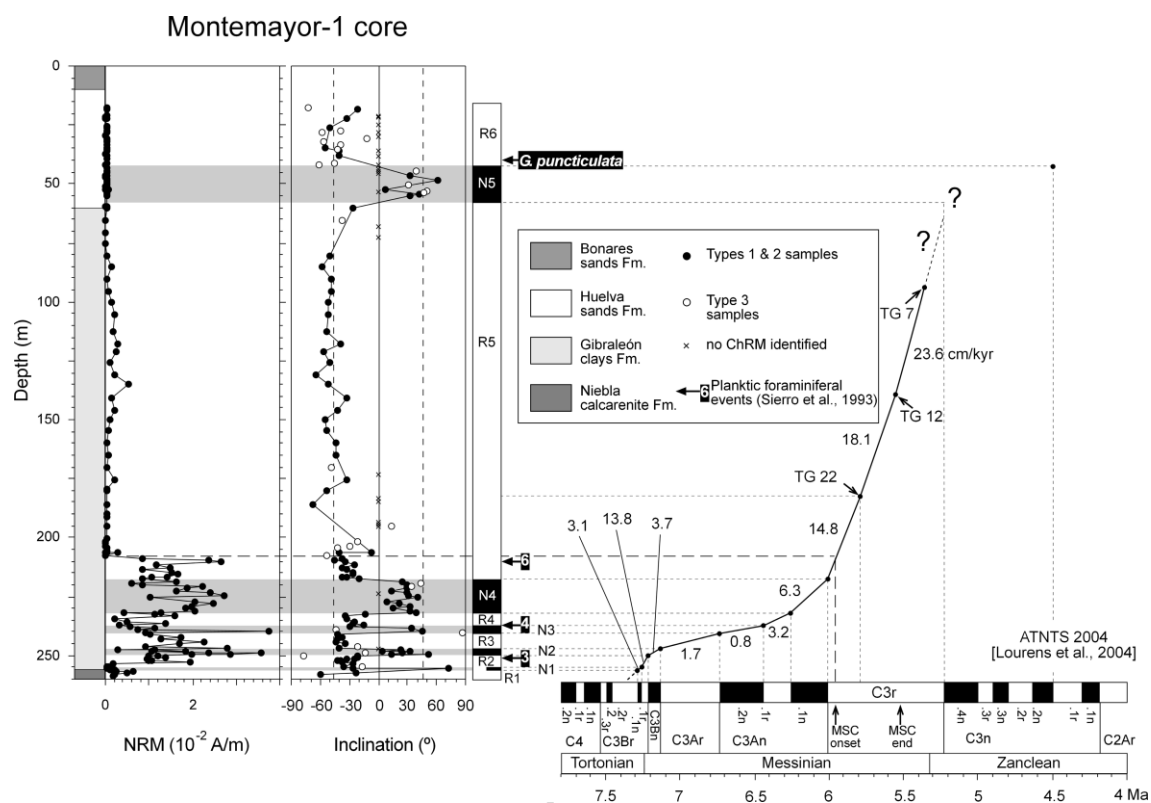


Figure 2

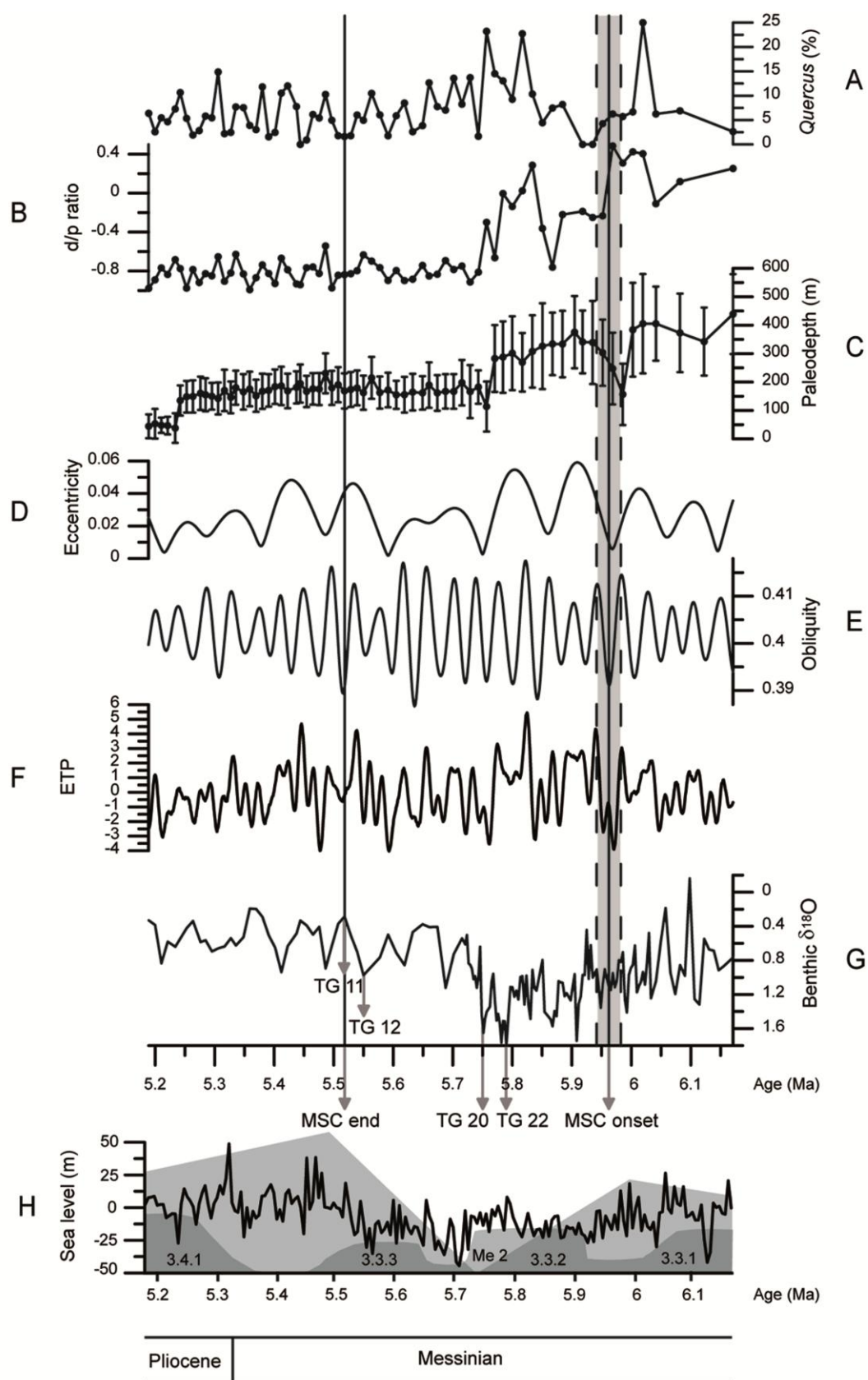


Figure 3

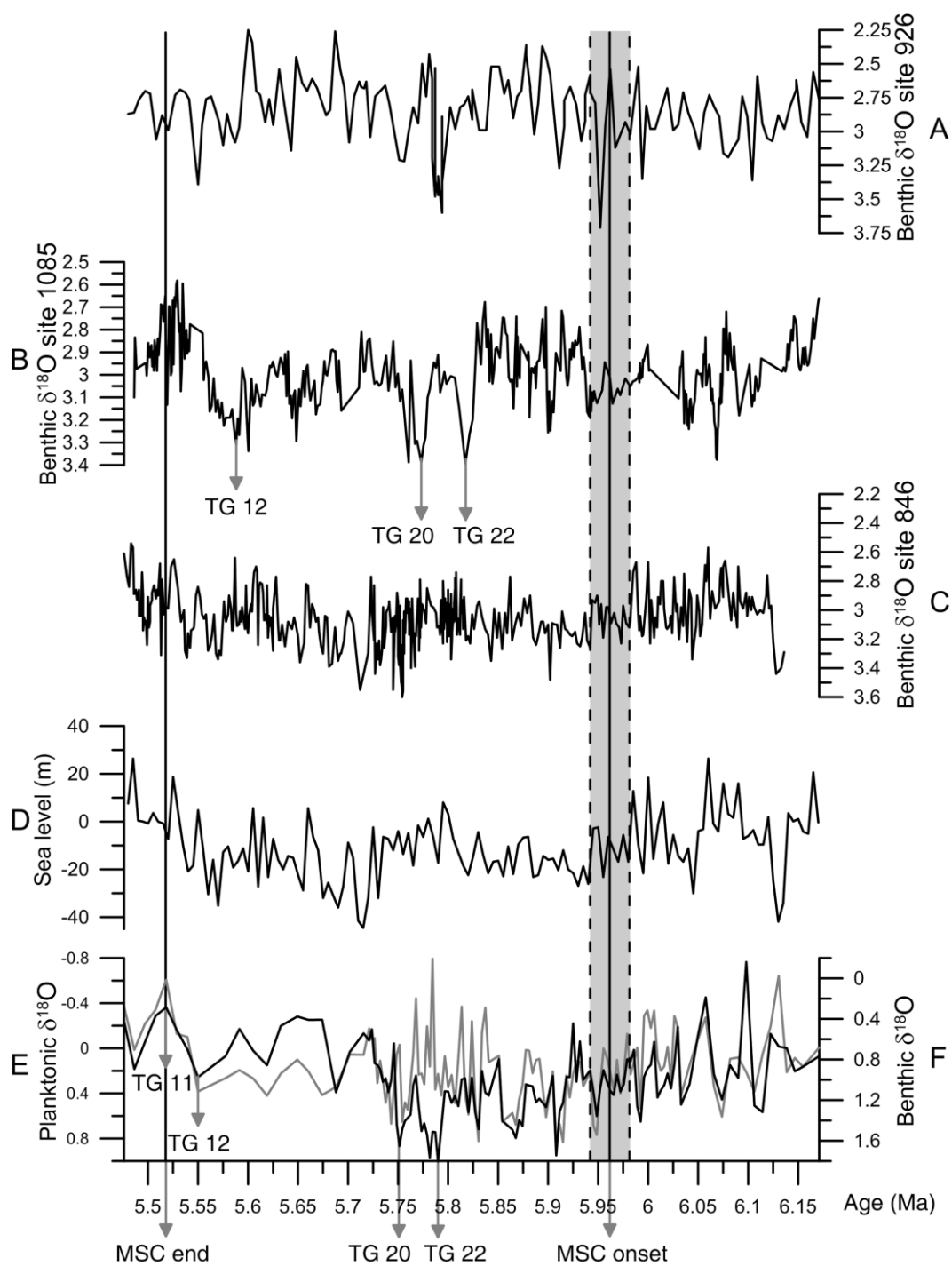


Figure 4

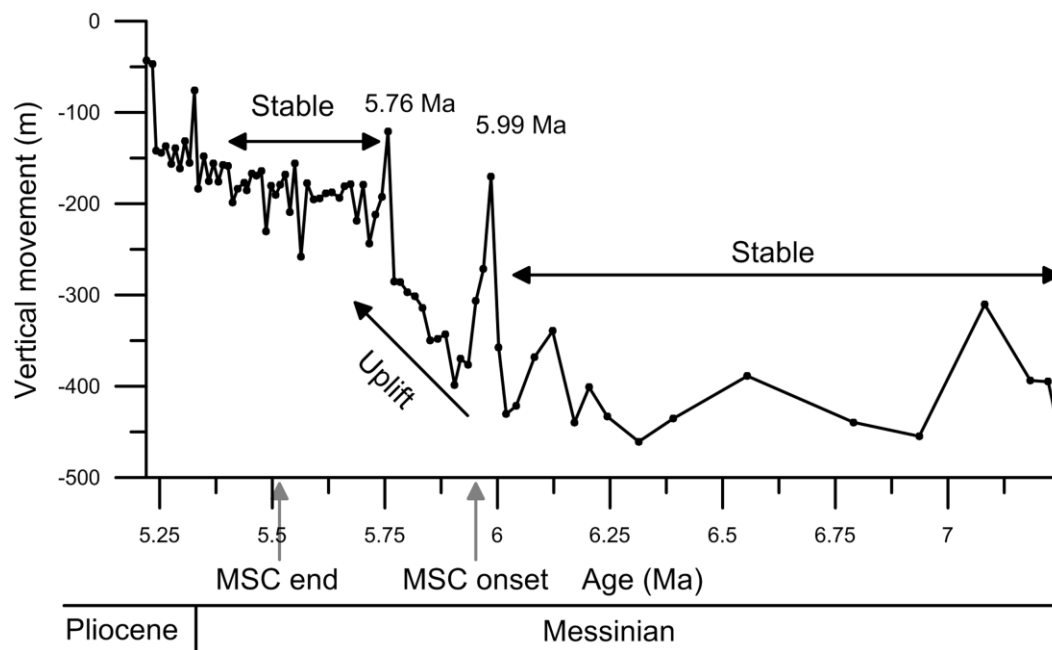


Figure 5

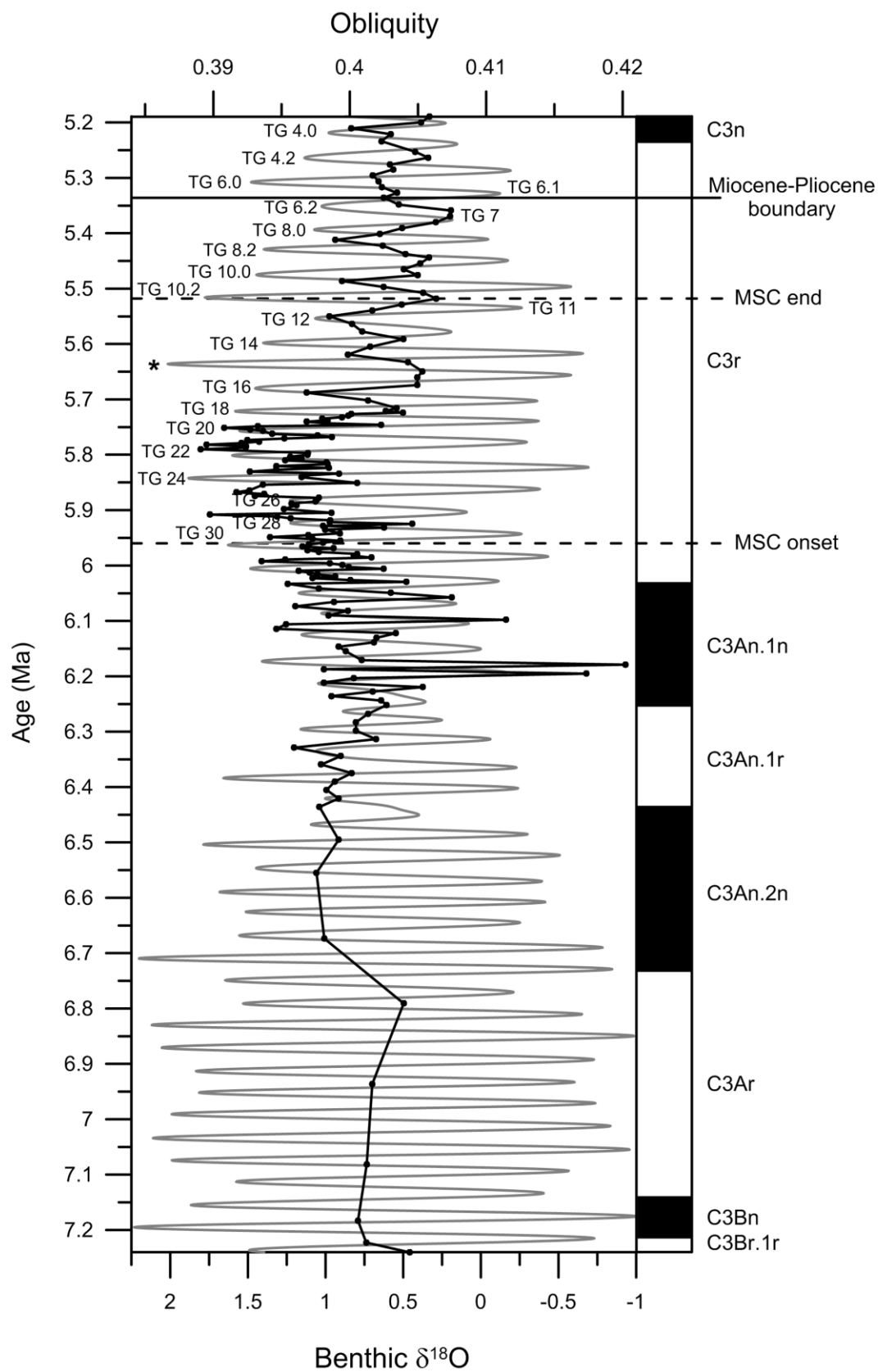


Figure 6

### Highlights

We study a complete Messinian Atlantic marine record from the Guadalquivir Basin.

The causes of the onset and cessation of the Messinian salinity crisis are analysed.

A glacioeustatic 60-m sea-level drop triggered the Messinian salinity crisis.

A two-step flooding model is proposed for the end of the Messinian salinity crisis.

A late Messinian glacioeustatic sea-level rise reinundated the Mediterranean.